2025 IEEE World Haptics Conference (WHC)
Suwon Convention Center, Suwon, Korea
July 8 ~ 11, 2025

Stiffness Perception Device Based on Skin-Stretch for Laparoscopic Surgery: Radial Palpation and Influence of the Fulcrum Effect

Charlélie Saudrais
ISIR
Sorbonne Université
CNRS
Paris, France
saudrais@isir.upmc.fr

Bernard Bayle
ICube
Université de Strasbourg
CNRS
Paris, France
bernard.bayle@unistra.fr

Doris da Silva
ISIR
Sorbonne Université
CNRS
Paris, France
dasilva@isir.upmc.fr

Marie-Aude Vitrani
ISIR
Sorbonne Université
CNRS
Paris, France
vitrani@isir.upmc.fr

Fabien Vérité
ISIR
Sorbonne Université
CNRS
Paris, France
verite@isir.upmc.fr

***Abstract*—Laparoscopic surgery benefits patients but adds complexity for surgeons due to perception limitations, especially haptic force perception degradation. This paper assesses the performance of a tactile feedback based on tangential skin-stretch to enhance radial force perception at the laparoscopic tool-tip and its ability to undistort the lever effect. Twelve novice participants conducted a palpation task that consisted in identifying the stiffest among three stiffness samples under three feedback modalities: no sensory augmentation, a visual bar-graph feedback, and the proposed tactile feedback. The results show that for a laparoscopic palpation task both visual and tactile feedback increase its success rate, and reduce the applied forces while not increasing the perceived workload, regardless of insertion depth variation. However, the skin-stretch feedback was the only one to improve performance on both objective and subjective metrics. The obtained results highlight the potential of skin stretch in enhancing force perception, while also serving as a reminder of the persistent challenge of force distortion due to the fulcrum effect in minimally invasive surgery.**

***Index Terms*—Laparoscopic surgery, fulcrum effect, stiffness perception, sensory augmentation, tactile feedback.**

I. Introduction

MINIMALLY invasive surgery (MIS), and in particular laparoscopic surgery, uses small incisions in the abdomen to allow inserting an endoscope and elongated tools through rubber sealed ports, called trocars. This surgical approach offers a multitude of advantages to the patient when compared to open surgery, including reduced post-operative pain, a shorter recovery time and less organ damages [1]. Nevertheless, these benefits have to be weighed against the higher gesture complexity faced by surgeons. This increased difficulty arises from limitations in perception, in particular the degradation of both visual perception and haptic perception of forces [2], [3]. Specifically, the visual perception is degraded due to the loss of depth perception, the reduction of the field of view and the difficult hand-eye coordination. Regarding the impairment of haptic perception, on the one hand, the axial stiffness of the abdominal wall and the friction of the trocar alter the axial perception of forces [4], [5]. On the other hand, the flexion of the elongated tools, the radial elasticity of the abdominal wall together with the fulcrum effect greatly contribute to distort the perception of radial forces [6].

It is important to highlight the particular role of the fulcrum effect, due to the mechanical constraints at the insertion point. It is twofold: radial movement inversion and scaling depending on the insertion of the tool, the latter being often referred to as lever effect. Niksy *et al.* [7] showed that the ratio between actual and perceived stiffness is the squared ratio between the inserted length and the external length of the tool. Therefore, not only can the perceived stiffness greatly differ from the real tissue stiffness, but the same tissue will have a different apparent stiffness depending on the insertion depth. This perception degradation could lead, among others, to tissue degradation caused by the application of excessive forces [8], [9] and poor palpation precision [10], resulting in a difficult assessment of tissue stiffness. Indeed, it has been reported that surgeons equally rely on visual and haptic cues, to assess the stiffness of the surgical environment [11]–[13]. Since these cues are distorted, it poses challenges in accurately evaluating tissues stiffness. In a practical context, this impairment of perception in MIS can lead to a higher error rate in comparison with open surgery. For instance in the case of laparoscopic cholecystectomy, studies have revealed that the incidence of injuries caused to the bile ducts is three times higher compared to open surgery [14] and this rate does not appear to decrease with experience [15]. Moreover, it was suggested that this increased injury rate is not related to errors in manipulation or lack of knowledge but rather to misinterpretation [16].

In comparison to robot-assisted minimally invasive surgery (RMIS), where the fulcrum effect can be eliminated with robotic assistance [17]–[19], addressing the fulcrum effect in manual MIS is not straightforward. Schmitt *et al.* [20] addressed the problem using the comanipulation paradigm in order to undistort the stiffness perception. In this approach, the handle, while still being held by the surgeon, is also attached to a robotic device. The device applies a force on the handle depending on the lever ratio in order to replicate the force measured at the end of the instrument. However, the initially promising results were limited by individual perception and by the influence of the feedback method on the gesture itself. Alternatively, Spiers *et al.* [21] presented a semi-robotic hand-held tool that cancels out the motion inversion caused by the fulcrum effect. An experimental study in a virtual environment

This work was supported by the *Investissements d'Avenir* program of the French Government, more specifically by Labex CAMI ANR-11-LABX-0004

showed faster skill acquisition. However the proposed solution cannot address the degradation of haptic perception.

Surgeons widely believe that rendering the real and undistorted forces to enhance perception would be pertinent [22]. In this regard, a proposed approach is to improve laparoscopic tools with either enhanced haptic feedback, active [23] or passive [24], or additional capabilities, such as measuring the stiffness of grasped tissues [25]. However, these innovations are dedicated to grasping tasks and do not extend to palpation tasks. Another appealing solution is sensory augmentation, which can be defined as using devices to assist a functional human sense by conveying pertinent information [26], [27], thereby augmenting the perception. Indeed, the sensory combination of natural feedback modalities, such as visual and haptic information, has been demonstrated to reduce variability and enhance performance [28]. Similarly, the sensory combination of artificial feedback modalities has also been proven more effective than when each information is provided individually [29]. Nonetheless, since the problem tackled in this work would involve the more challenging context of augmenting natural but degraded information with artificial but precise information, the previous findings can not be directly extended and must be investigated. Several researchers suggested relying on the visual modality to augment the force perception, rendering the palpation force as a graph [30], or as a map, either 2D [31] or 3D [32]. However, to limit the load on the visual modality, which is already heavily solicited [2], tactile feedback appears as a more suited alternative. Vibrotactile force feedback has been widely studied for laparoscopic surgery, either directly in the hand [33] or delocalized to prevent disturbing the gesture and provided on the upper arm [34], under the foot [35], or in the opposite hand as the one holding the tool [36]. Although vibrotactile feedback offers several advantages, such as compactness and lightweight design, its stimulus interpretation can sometimes be ambiguous, potentially affecting its effectiveness in certain applications [37].

Skin deformation-based feedback is an alternative approach to augmenting force information. Fukuda *et al.* [38] proposed a 1DoF ring applying pressure around the finger to render the tooltip force, a concept later enhanced by Ly *et al.* [39] with a 3DoF variant. Although not explored in conventional laparoscopic surgery, tangential skin deformation – skin stretch – applied on the fingerpad has shown significant potential as a substitute for force feedback in teleoperation [40]–[43]. In addition, Quek *et al.* [44] demonstrated that adding skin stretch to non-degraded force feedback can amplify or reduce the perceived stiffness. However, providing skin-deformation feedback at the hand might disturb the medical gesture. A solution to address this problem is to delocalize the feedback. Fukuda *et al.* [45] proposed applying a normal force on the user's foot to render the applied force. Alternatively, Tanaka *et al.* [46] proposed a wrist-worn device rendering the force applied at the tooltip by normally indenting the skin. In a different context, skin stretch wristbands have been widely studied and proved beneficial for navigation [47], or for proprioceptive feedback for prostheses [48]. The present study explores the use of skin deformation-based feedback applied to the forearm via a wristband device. This approach ensures minimal interference with surgical gestures while integrating feedback directly into the palpation movement. Tangential skin-stretch feedback is employed instead of normal skin deformation, leveraging its intuitive nature [49] and the higher sensitivity of forearm skin to tangential displacement compared to normal displacement [50]. In [51], we carried out a preliminary study that demonstrated the potential of a wristband providing skin-stretch feedback in an axial palpation context, where force perception was primarily impaired by trocar friction. The study yielded promising results as the skin-stretch outperformed conventional visual bar-graph feedback and no feedback in terms of stiffness perception accuracy. However, it did not address the more complex scenario of radial palpation, which introduces additional challenges, including the fulcrum effect and the elasticity of the abdominal wall. Unlike axial forces, where deformation and force are collinear, radial forces introduce non-collinearity, potentially complicating feedback interpretation and increasing cognitive load. To address these limitations, the present study evaluates the ability of our wristband to augment degraded and distorted natural force perception with delocalized tangential skin-stretch feedback in the challenging context of radial palpation. The structure of the paper is as follows: the design and performance of the device are detailed in Sec. II. Sec. III presents an experimental evaluation, followed by the results in Sec. IV and a discussion in Sec. V, including conclusions and future perspectives.

II. Skin-Stretch Wristband: Design & Control

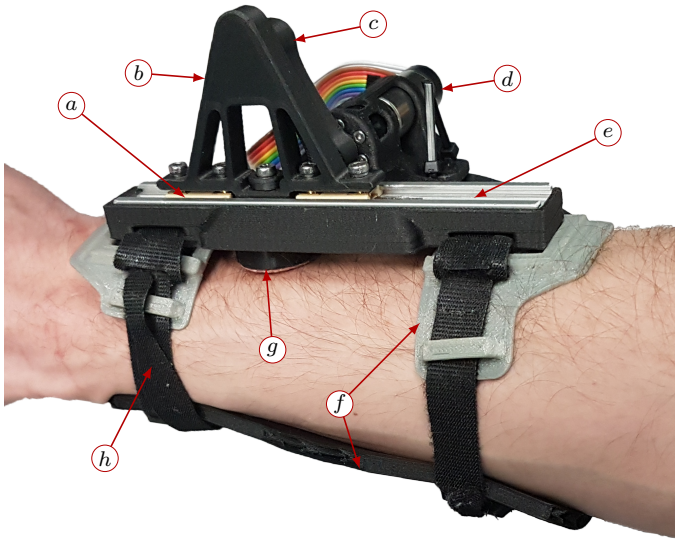

Fig. 1. Skin-stretch wristband: (a) low-friction carriage, (b) slider, (c) crank, (d) motor, (e) guide rail, (f) soft TPU pads, (g) tactor, (h) hook-and-loop fasteners

A. Mechanical Design

We implemented a wristband-based skin stretch device to evaluate the proposed strategy. The system, placed on a user's forearm, is pictured in Fig. 1. This 1-DoF device consists of a Scotch-Yoke mechanism, a variant of the crank-slider in which a crank (c) with a pin that engages in a slot of a sliding yoke (b) transforms the rotational motion of the motor (d) into a linear motion. A rigid 3D-printed housing incorporates the motor (d) and the guide rail (e) on which two carriages (a) attached to the slider translate. A hemispherical tactor (g) is connected to the slider by means of spring-based mechanism, to ensure continuous contact with the forearm. This tactor, in contact with the skin, is the end-effector providing the skin-stretch. The device is secured on the arm using soft TPU pads strapped together. The design of the prototype was performed following the guidelines provided by Gleeson *et al.* [52]. Specifically, the skin deformation being friction induced, it is crucial to avoid slippage. Therefore, the tactor is coated with high-friction silicone rubber presenting a rough texture. It features a large diameter of $25\,\mathrm{mm}$. Moreover, due to the upper pads solely resting against the skin at the extremities of the rail, the arm restraint is partially opened, allowing the skin surrounding the stimulation area to move freely. Lastly, the mechanism is powered by Maxon brushless DC motor EC-Max 16, with a 19:1 planetary gearbox and its position is measured by a 512 counts per turn encoder. The device features a $\pm 20\,\mathrm{mm}$ range from the center position. It is able to provide a maximum tangential force of $2.5\,\mathrm{N}$ and the maximum linear speed of the end effector is $1.4\,\mathrm{m{\cdot}s^{-1}}$.

B. Device Control

The desired end-effector position, i. e. the skin-stretch tactor tangential displacement, rendering the force information is calculated similarly to [42], [49] as follows:

$$x = r_{ss} f, \tag{1}$$

where x [m] is the desired position of the skin-stretch tactor, r_{ss} [m/N] is the skin stretch ratio (also referred to as the deformation-to-force ratio) and f [N] is the measured force to be rendered. The desired position of the effector is then converted into a desired motor angle through the mechanism kinematic mapping. The control law requires the motor to be position-controlled. This is performed by a Maxon EPOS4 digital positioning controller. The force to be rendered by the device is acquired by a force/torque sensor (ATI Nano17 SI-50-0.5) placed at the end of the laparoscopic instrument. Lastly, all the instrumentation and control signals are interfaced to a single-board master computer running a real-time controller operating at $1\,\mathrm{kHz}$.

C. Evaluation of System Performance

System performance was evaluated by measuring the static backlash, useful bandwidth, and tracking error. The backlash of the mechanism was assessed with a mechanical comparator. The tactor was moved over the entire operating range under varying loads. The largest backlash measured was $0.158\,\mathrm{mm}$.

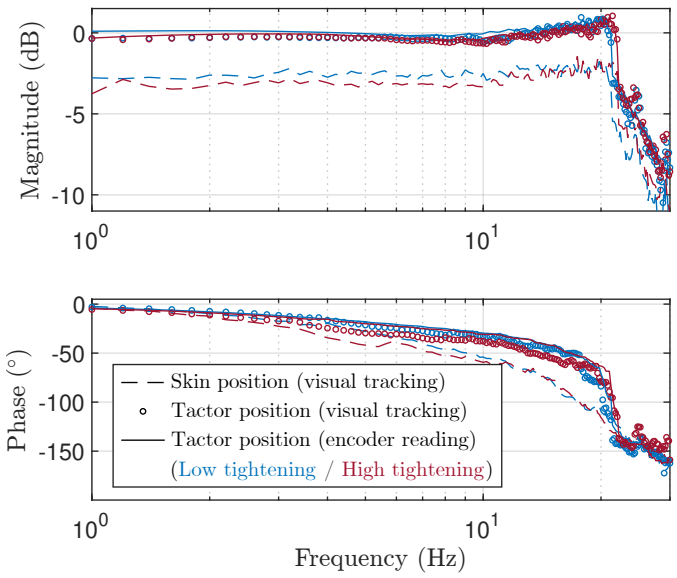

Fig. 2. Experimental Bode diagram. The figure shows the amplitude ratio of the tactor position assessed using both visual tracking and the motor encoder, as well as the skin position recorded by visual tracking. All blue (resp. red) curves refer to the application of a low (resp. high) tightening force of the wristband around the wrist.

In addition, the frequency response of the system was evaluated in order to determine the usable bandwidth. The wristband was tightened on the forearm and positioned as shown in Fig. 1. The end-effector was controlled to follow a sinusoidal trajectory of $20\,\mathrm{mm}$ peak-to-peak amplitude with a frequency ranging from 1 to $30\,\mathrm{Hz}$ by $0.2\,\mathrm{Hz}$ steps. The experimental Bode diagram, representing the input-to-output position of the device, is presented in Fig. 2. The position of the tactor shows a cut-off frequency of approximately $20\,\mathrm{Hz}$. However, as a small resonance is observed in the region from 10 to $20\,\mathrm{Hz}$, we consider the usable frequency range to be 0 to $10\,\mathrm{Hz}$. This range is characterized by a $0\,\mathrm{dB}$ amplitude ratio and a phase lag that exhibits a linear decrease of about 3 degrees per hertz. The position of the tactor, whether recorded by visual tracking or calculated using the motor encoder, is consistent, which justifies the validity of using the motor position to evaluate the effector position. Also, the position of the skin surrounding the tactor was visually tracked to ensure the proper transmission of the end-effector displacement to the skin. The Bode diagram confirms that the stretched skin features the same dynamics. The magnitude offset and the degraded phase lag are most likely due to the fact that the tracked skin is on the side of the effector, thus, not the one in direct contact with the tactor. Moreover, the performances are similar regardless of the tightening force of the wristband fasteners. Only a slight degradation in performance can be noted when increasing the tightening force. Lastly, the tracking position error, assessed on the usable frequency range, was the highest at $10\,\mathrm{Hz}$, i. e. the maximum frequency, with a value of $5.2\,\mathrm{mm}$, around $25\,\%$ of the workspace.

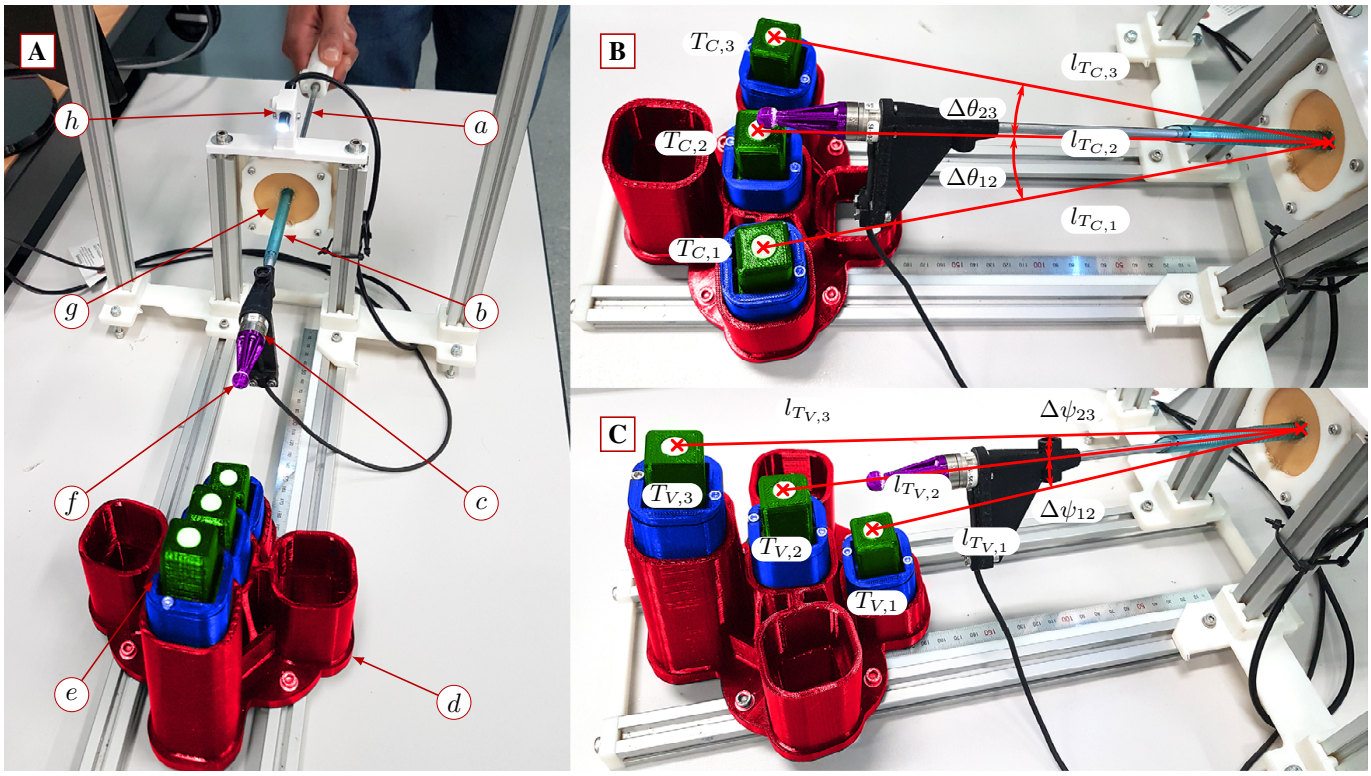

Fig. 3. Experimental setup of the study – Distal side (the image has been colorized for clear identification of each part): A: (a) tool, (b) tocart, (c) F/T sensor, (d) stiffness sample holder, (e) stiffness samples (base in blue, slider in green), (f) spherical palpation probe, (g) abdominal wall, (h) camera – B: Samples at constant depth – C: Samples at variable depth

III. Experimental Methods

An experimental protocol was designed in order to evaluate the ability of our approach to augment the perception of radial forces and undistort the lever effect. This method was compared to a conventional visual feedback and to no feedback augmentation. The experiment was a stiffness discrimination task in which the participants, presented with three stiffness samples, were asked to identify the stiffest one. The task was performed under conditions mimicking laparoscopic surgery.

A. Participants

We recruited a total of 12 participants (4 females, 8 males) between the ages of 22 and 30 years old. Although participants had different levels of experience with haptic interfaces, none of them reported recent experience with either skin-stretch feedback or laparoscopic surgery. All participants provided informed consent and the experimental study was carried out in accordance with the ethical principles provided by the declaration of Helsinki, and was approved by the local Research Ethics Board.

B. Experimental Setup

The experimental setup used for the study is presented in Fig. 3 and 4. In particular, Fig. 3 depicts the distal side of the experimental setup, and Fig. 4 presents the proximal side from the participant's point of view. On the one hand, it consists of a tool (*a*) equipped with a palpation probe (*f*, purple) placed in a trocar (*b*), itself inserted in a mock abdominal wall (*g*) and, on the other hand, there is a sample holder (*d*, red) containing three stiffness samples (*e*, base in blue and slider in green). A reference system (F, x_0, y_0, z_0) is represented in blue in Fig. 3 to ease the description of the motion of the tool.

The palpation tool consists of a $\varnothing 5\,\mathrm{mm} \times 300\,\mathrm{mm}$ aluminum rod, equipped with a cylindrical handle on one side and a force/torque sensor (*c*, ATI Nano17 SI-50-0.5) on the other side. In order to interact with the environment a $\varnothing 10\,\mathrm{mm}$ indentation spherical probe is attached on the tool adapter plate of the force sensor. This tool features a total length of $500\,\mathrm{mm}$.

The fulcrum constraint is enforced by the trocar (by Applied®) inserted into a silicone pad from a LaproTrain (by Endosim®) that mimics the abdominal wall. The palpation instrument is able to rotate in 3D and to translate along its longitudinal axis. The tool and trocar assembly is fixed at the front of the base frame of the setup as depicted in Fig. 3-A and 4.

At the distal side of the setup, the sample holder, placed at the other end of the setup frame, contains three stiffness samples. The design of the stiffness sample is based on a prismatic joint integrating a calibrated spring, characterized by its stiffness K, between the slider, colored in green, and the base, colored in blue. In addition, the sample holder contains five slots and allows two configurations: the samples are either positioned at a constant insertion depth, as in Fig. 3-B or at varying depth, as in Fig. 3-C. In the former

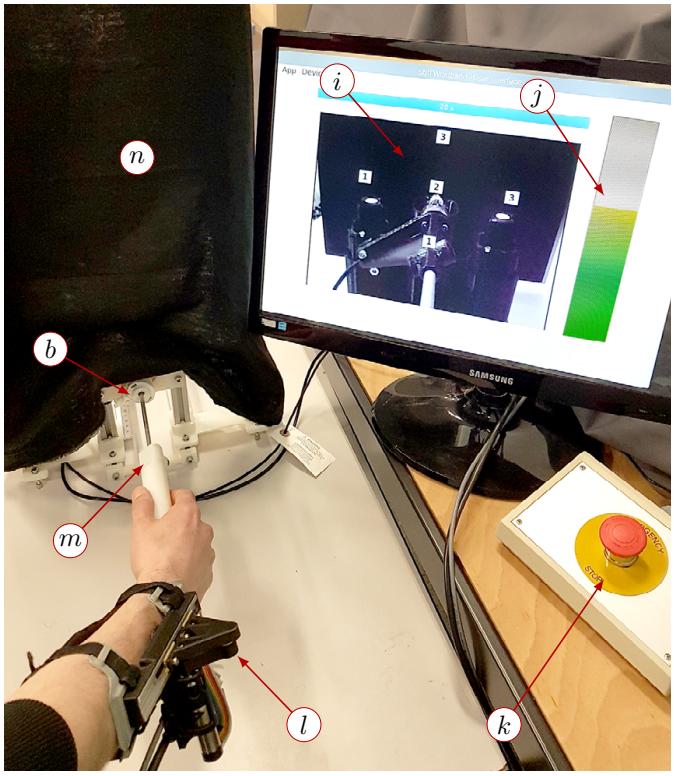

Fig. 4. Experimental setup of the study – Proximal side: (b) trocar (i) view of the scene, (j) force gauge (visual feedback), (k) emergency stop, (l) skin-stretch device, (m) tool, (n) opaque sheet

configuration, the three samples, identified by the points $T_{C,i}, i \in \{1,2,3\}$, positioned at the center of their upper face, are placed at a constant distance l_T from the fulcrum point F, i. e. $l_{T_{C,1}} = l_{T_{C,2}} = l_{T_{C,3}}$. The lever ratio is constant, i. e. the apparent stiffness of a sample is the same in all three positions. To navigate from one sample to another, the user only needs to perform a rotation $\Delta\theta$ about $(F, \boldsymbol{z}_0)$. In the latter configuration, the three samples, now identified by the points $T_{V,i}, i \in \{1,2,3\}$, are positioned at a varying depth from the fulcrum point, $l_{T_{V,1}} < l_{T_{V,2}} < l_{T_{V,3}}$. The lever ratio is then different depending on the sample position. In other words, the apparent stiffness of a sample depends on its position. In order to navigate from one sample to another, the user needs to translate the tool along its longitudinal axis. Also, to prevent the tool from colliding with the preceding samples, a small rotation $\Delta\psi$ is required about $(F, \boldsymbol{y}_0)$. Finally, the sample holder is designed so that, when the center of the palpation probe is positioned in $T_{C,i}$ and $T_{V,i}, i \in \{1,2,3\}$, the translational axis of the considered stiffness sample is perpendicular with the longitudinal axis of the tool. Therefore, for both fixed and variable insertion depth, the user only needs to perform a swinging motion to indent each sample.

At the proximal side of the setup, see Fig. 4, a dark opaque sheet (*n*) prevents the direct view of the scene. Instead, in order to replicate the view offered by a fixed endoscope, the scene is filmed by a camera (*h*), visible on Fig. 3-A, and displayed on a screen (*i*).

C. Experimental Task

The elementary task, inspired by [20], [45] is a palpation task in which the participant, holding the tool, interacts with three stiffness samples. Two of these samples, the *references*, feature the same stiffness $K_{ref} = 65\,\mathrm{N{\cdot}m^{-1}}$, and one, the *odd-one-out*, stiffer than the *references* features a stiffness $K_o = 90\,\mathrm{N{\cdot}m^{-1}}$ except for the practice session where $K_o = 180\,\mathrm{N{\cdot}m^{-1}}$. These stiffness values were chosen for the following two reasons: 1) they are comparable to the ones used in palpation experiments focusing on the impact of the fulcrum effect on stiffness perception [7], and 2) the forces obtained with these samples correspond to the forces applied in the context of cardiothoracic and general surgery [53]. The goal of the task, replicating the detection of tumors, is to identify the position of the *odd-one-out*. As it has been proven that surgeons rely on both haptic and visual cues to assess tissues stiffness [7], [12], when the tool is in contact with a sample, an overlaying black rectangle hides both the tool and the samples. Since our objective in this study is only to focus on the haptic perception, it ensures that the participant can no longer rely on additional visual cues.

D. Conditions

This elementary task is performed at both *constant* and *variable* insertion depth for each of the following modalities:

- *Control*. Participants perform the task relying solely on the haptic feedback associated with the natural perception, without any additional sensory augmentation. This condition serves as the baseline for comparison.
- *Visual*. Participants rely on the natural haptic feedback that is augmented by a visual force feedback. This visual feedback is presented as a colored vertical bar graph on the user interface, located to the right of the view of the scene. It is always and easily visible. The height of the bar graph corresponds to the force at the tool-tip, in $[0\,\mathrm{N}; F_{\max} = 2\,\mathrm{N}]$. The color of the bar graph changes in accordance with the measured force value. This type of conventional visual feedback, commonly employed in the literature, e.g. similar to the one used in [29], serves as a suitable benchmark for comparing against other feedback modalities.
- *Skin-stretch*. Participants rely on the natural haptic feedback augmented by the tactile feedback detailed in II provided through a tangential skin deformation applied to the arm using our device. The displacement of the tactor is proportional to force measured at the tool-tip. The skin-stretch ratio was set at $r_{ss} = 12\,\mathrm{mm{\cdot}N^{-1}}$, covering a restitution range of $[0\,\mathrm{N}; F_{\max} = 2\,\mathrm{N}]$.

To optimize the deformation range and prevent saturation, a preliminary study conducted with participants distinct from those involved in the current study, aimed to fine-tune the skin stretch ratio r_{ss}. In particular, the skin-stretch ratio was adjusted based on the average peak force exerted by participants to maximize resolution while avoiding saturation. In addition, to ensure a fair comparison between tactile and visual

feedback conditions, the restitution force range is identical. Furthermore, the stiffness difference between K_o and K_{ref} was adjusted based on pilot studies conducted exclusively under the *control* condition. These studies helped identify stiffness values that corresponded to a success rate of $50\,\%$ at a constant depth. Based on an estimation of the variability in participants' success rates, this $50\,\%$ threshold was set to yield the highest possible difficulty level while ensuring that no participant would be at the chance level. This ensures a proper comparison between the feedback modalities studied and the control condition.

E. Experimental Design

The experiment follows a $[2 \times 3]$ within-subject repeated measures design with the following 2-levels and 3-levels factors presented in subsection III-D:

- Insertion depth – *Constant* and *Variable*.
- Feedback modality – *Control*, *Visual* and *Skin-stretch*.

For each depth condition, there is one experimental block, subdivided into three sub-blocks, one per feedback modality. Each sub-block is divided into two parts: a training part of 3 repetitions and a main part of 10 repetitions. The initial practice session helped participants to familiarize themselves with the feedback conditions and the experimental setup. These experimental blocks and sub-blocks are presented in randomized order.

The experiment following a within-subject design, participants complete all combinations of factor levels, for a total of 78 repetitions. A brief break between the two blocks was therefore imposed to limit fatigue. The whole experiment lasted approximately 45 minutes for each participant.

F. Procedure

After reading written instructions regarding the objectives of this research and the course of the experiment, participants were given instructions to treat the following two constraints with equal importance: 1) complete each trial in the least amount of time and 2) apply only the force necessary to locate the stiffest sample, i. e. no excessive force. During the experiment, participants were standing, facing both the tool handle and the monitor displaying the view of the scene. For each trial, they were allowed to interact a maximum of three times with each sample and they were given 30 seconds. The timer started when they began interacting with a sample and stopped when they gave their answer. If the time limit was exceeded they were to stop immediately. They were also asked to rate the confidence in their answer. Then, during the practice session only, the participants were informed of the correct answer to provide feedback.

G. Metrics

The metrics used to assess the performance of the participants in the experiment are the following:

- *Success rate*. Number of correct identifications of the stiffest sample divided by number of trials.
- *Peak force*. Maximum palpation force applied.
- *Completion time*.
- *Confidence level*. Participants' confidence in their response, on a scale from 1 to 10, 10 being a very confident response.

Moreover, at the end of every sub-block, i. e. for each combination of factor, the cognitive load was evaluated using the NASA Raw Task Load Index (NASA-TLX), a subjective survey that assesses the perceived workload [54]. Lastly, participants were invited at the end of the experiment to fill out a 6-questions survey, evaluating their experience with the device and its understandability.

H. Data Analysis

The performance metrics as well as the cognitive load were analyzed carrying out two-way repeated measures (2RM) ANOVAs. Data was screened for outliers with respect to Mahalanobis criteria [55] and was screened for assumptions as follows. All data passed the normality assumption assessed with the Shapiro-Wilk test. In case of violation of the sphericity assumption evaluated with Mauchly's test, a correction was applied, either Huynh-Feldt or Greenhouse-Geisser depending on the value of the estimate of sphericity. Whenever at least one effect was found significant, posthoc tests whose nature depended on the significance of the interaction were carried out.

In case of a non-significant interaction, the main effects were analyzed as follows. When the effect of the feedback modality was significant, pairwise comparisons of the estimated marginal means (EMM) of each level of the factor were performed using Fischer's Least Significant Difference (F-LSD). However, when the effect of the insertion depth was significant, since it is a two-level factor, post-hoc analysis consisted in the direct comparison of the EMM. Otherwise, interaction plots were created to understand the nature of the interaction and for each significant factor, pairwise T-Test between all levels combinations were performed, at each level of the other factor.

For all the analyses considered, the statistical significance was set at 0.05. Whenever multiple comparisons were performed, the Holm-Bonferroni (H-B) correction was applied to prevent inflation of the family-wise error rate. Results are reported as follows for ANOVA: F(between groups degrees of freedom, within groups degrees of freedom) = $\mathrm{F}_{\mathrm{value}}$, p = p_{value}, η^2_{ges} = generalized eta squared. Marginal means are reported as M = marginal mean, SD = standard deviation. Statistical computing and graphics were realized with R [56].

IV. Results

Fig. 5 to 8 show the results for the performance metrics (success rate, peak force, confidence and completion time respectively). For each of these figures, the same data is reported twice with different grouping methods to better visualize the effect of each factor (feedback modality and insertion depth) or the interaction, if any. In particular, in the absence of interaction, the mean and standard error are overlayed on top of the boxplot to explicit the main effects while, if a significant

TABLE I
MEAN AND STANDARD DEVIATION FOR SUCCESS RATE ([0 1]), PEAK FORCE (IN N), CONFIDENCE ([1 10]) AND COMPLETION TIME (IN S)

	Mean / Standard Deviation				
	Feedback Modality			Insertion Depth	
	Control	*Visual*	*Skin-stretch*	*Constant*	*Variable*
Success Rate	0.50 / 0.13	0.67 / 0.13	0.73 / 0.14	0.69 / 0.15	0.58 / 0.16
Peak Force	2.00 / 0.95	1.33 / 0.42	1.28 / 0.36	1.41 / 0.55	1.66 / 0.82
Confidence	5.50 / 1.51	5.68 / 1.62	6.50 / 1.40	6.16 / 1.54	5.63 / 1.54
Completion Time	15.32 / 3.18	15.07 / 3.29	15.19 / 2.96	14.27 / 3.00	16.11 / 2.98

TABLE II
POST-HOC: P-VALUES OF SIMPLE EFFECTS FOR SUCCESS RATE.
LEFT TABLE: EFFECT OF THE INSERTION DEPTH FOR EACH FEEDBACK; RIGHT TABLES: EFFECT OF THE FEEDBACK FOR EACH INSERTION DEPTH

Comparison	*p-value*
Control / *Constant* vs *Variable*	**0.0023**
Visual / *Constant* vs *Variable*	0.29
Skin-stretch / *Constant* vs *Variable*	**0.0040**

	Comparison	*p-value*
Constant	*Control* vs *Visual*	**0.034**
	Control vs *Skin-stretch*	**<0.001**
	Visual vs *Skin-stretch*	**0.034**

	Comparison	*p-value*
Variable	*Control* vs *Visual*	**<0.001**
	Control vs *Skin-stretch*	**<0.001**
	Visual vs *Skin-stretch*	0.55

TABLE III
POST-HOC: P-VALUES OF MAIN EFFECT FOR PEAK FORCE, CONFIDENCE AND COMPLETION TIME

Comparison	p-value		
	Force	*Confidence*	*Time*
Constant vs *Variable*	**0.019**	**0.025**	**0.0057**
Control vs *Visual*	**0.011**	0.47	1.00
Control vs *Skin-stretch*	**0.044**	**0.0018**	1.00
Visual vs *Skin-stretch*	0.77	**0.012**	1.00

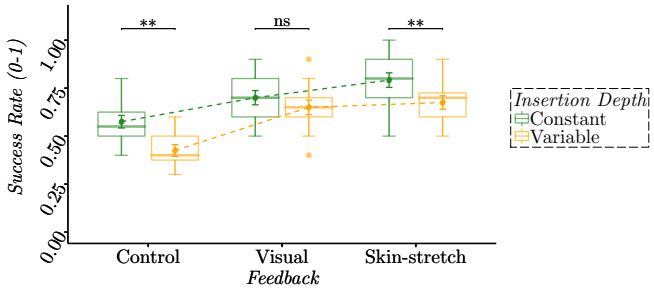

(a)

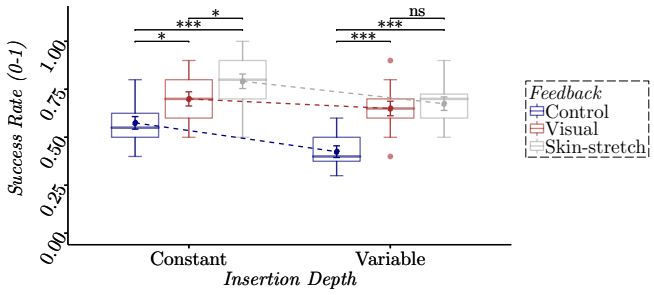

(b)

Fig. 5. Experimental results for the success rate. (a) Feedback modality on the x-axis and insertion depth by color scale (b) Insertion depth on the x-axis and feedback modality by color scale. Post-hoc pairwise T-Tests with Holm-Bonferroni correction p-values are indicated as follows: ns $= p > 0.05$, * $= p < 0.05$, ** $= p < 0.01$, *** $= p < 0.001$

interaction is present, interaction plots (means and standard errors of each factor combination) are displayed to facilitate the analysis. Fig. 9 reports the results for the cognitive load and Fig. 10 presents the results for the perceived difficulty. All figures use the same color code, which is defined as follows: blue, red, light gray refer to the feedback modalities control, visual, skin-stretch respectively and green, yellow refer to the insertion depth constant and variable respectively. For the post-hoc analysis of all performance metrics, M and SD are reported in Tab. I. The *p*-values are shown in Tab. II for the success rate and in Tab. III for the other performance metrics.

A. Success Rate

Fig. 5 shows the mean success rate for each combination of feedback modality and insertion depth. Both the feedback modality and the insertion depth had a significant effect on the success rate ($F(2, 22) = 22.95$, $p < 0.001$, $\eta^2_{ges} = 0.418$ and $F(1, 11) = 14.44$, $p = 0.0030$, $\eta^2_{ges} = 0.169$ respectively). Although the effect of the interaction was not statistically significant, the interaction graphs overlayed on top of the boxplot suggest the presence of an interaction. In this context, since the ANOVA might just fail to detect the interaction, it is advised to conduct posthoc tests as if an interaction were present [57]. Therefore, for each factor, dependent pairwise T-tests with an H-B correction were performed between all level combinations, at each level of the other factor. On the one hand, the supposed interaction was studied focusing on the feedback modality. Regarding the control condition, the success rate was lower than with augmented feedback, whatever the insertion depth. At a constant depth, the control success rate was 17.2% (0.12) smaller than the visual success rate and 25.6% (0.21) lower than the skin-stretch success

rate. At a varying depth, the control success rate was 33.8% (0.22) lower than the visual success rate and 36.7% (0.25) less than the skin-stretch success rate. However, regarding the augmented feedback modalities, while, at a constant depth, the skin-stretch success rate was 11.4% (0.09) better than the visual success rate, at a varying depth, there was no significant difference between the visual success rate and the skin-stretch success rate, which confirms the presence of an interaction. On the other hand, this interaction was also studied focusing on the insertion depth. One can notice that varying the insertion depth led to a significant success rate decrease of 25.9% (0.15) for the control condition and 13.9% (0.11) for the skin-stretch feedback. However, the visual success rate was not significantly impacted. All p-values are reported in Tab. II.

B. Peak Force

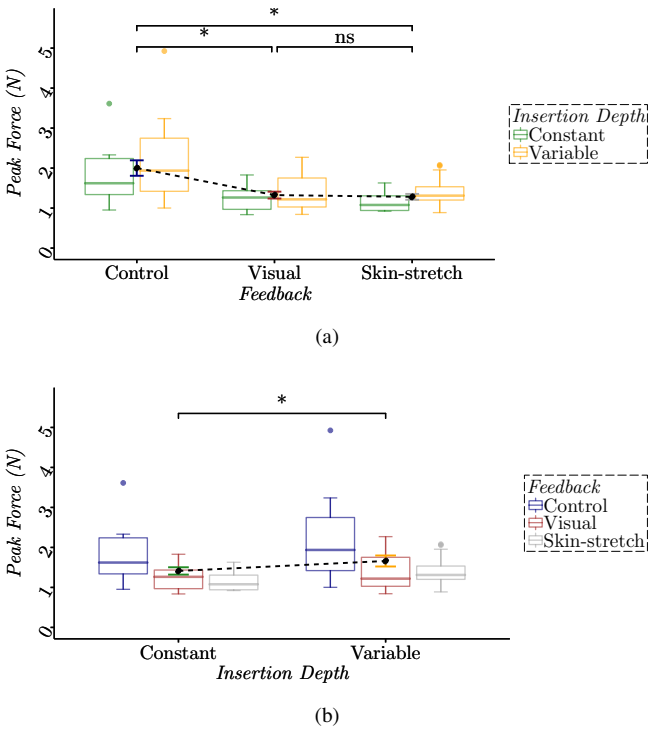

Fig. 6. Experimental results for the peak force. (a) Feedback modality on the x-axis and insertion depth by color scale (b) Insertion depth on the x-axis and feedback modality by color scale. Post-hoc pairwise comparisons of the EMM using Fischer's LSD p-values are indicated as follows: ns $= p > 0.05$, * $= p < 0.05$

Fig. 6 presents the mean peak force for each combination of experimental conditions. The effect of the feedback modality was significant as well as the effect of the insertion depth ($F(2, 22) = 7.60$, $p = 0.0031$, $\eta^2_{ges} = 0.229$ and $F(1, 11) = 7.56$, $p = 0.019$, $\eta^2_{ges} = 0.041$ respectively). The interaction was found to be not significant. Regarding the effect of the feedback modality, no significant difference was found between the skin-stretch feedback and the visual feedback. However, in comparison with the control feedback, the peak force applied was significantly lower with both the skin-stretch feedback with a 36.0% (0.72 N) decrease and the visual feedback with a 33.5% (0.67 N) decrease. As far as the effect of the insertion depth is concerned, varying the insertion depth led to a significant augmentation of the peak force, with a 17.7% (0.25 N) increase. The p-values are reported in Tab. III.

C. Confidence Level

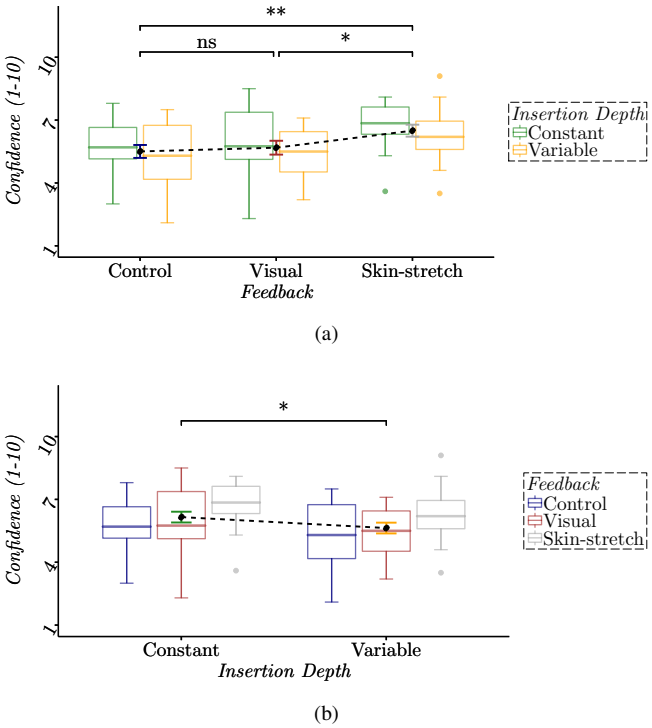

Fig. 7. Experimental results for the confidence level (1-10). (a) Feedback modality on the x-axis and insertion depth by color scale (b) Insertion depth on the x-axis and feedback modality by color scale. Post-hoc pairwise comparisons of the EMM using Fischer's LSD p-values are indicated as follows: ns $= p > 0.05$, * $= p < 0.05$, ** $= p < 0.01$

Fig. 7 shows the mean confidence level for each combination of factors. The effects of both the feedback modality and the insertion depth were significant ($F(2, 22) = 10.56$, $p < 0.001$, $\eta^2_{ges} = 0.081$ and $F(1, 11) = 6.75$, $p = 0.025$, $\eta^2_{ges} = 0.031$ respectively). The interaction was not significant. On the one hand, regarding the effect of the feedback modality, there was no significant difference between the control condition and the visual feedback. Nonetheless, with the skin-stretch feedback, subjects were significantly more confident than with both the control feedback, with a 18.2% (1.00 point) increase, and the visual feedback, with a 14.4% (0.82 point) increase. On the other hand, regarding the effect of the insertion depth, participants were significantly less confident with a variable insertion depth compared to a constant insertion depth with about 8.6% (0.53 point) decrease. All p-values are reported in Tab. III.

D. Completion Time

Fig. 8 depicts the average completion time for each combination of feedback modality and insertion depth. A 2RM ANOVA revealed a significant effect of the insertion depth

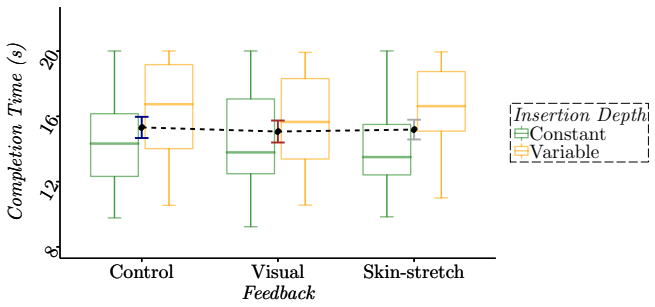

(a)

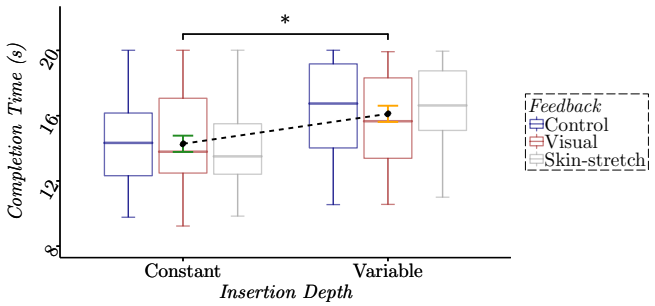

(b)

Fig. 8. Experimental results for the completion time. (a) Feedback modality on the x-axis and difficulty level by color scale, no significant differences were observed between the three conditions. (b) Difficulty level on the x-axis and feedback modality by color scale. Post-hoc pairwise comparisons of the EMM using Fischer's LSD p-values are indicated as follows: * = $p < 0.05$.

($F(1, 11) = 11.73$, $p = 0.0057$, $\eta^2_{ges} = 0.089$). However, the effects of both the feedback modality and the interaction were not statistically significant. With a variable insertion depth, participants were significantly slower to perform the task in comparison with a fixed insertion depth with a 12.9% (1.84 s) increase. Post-hoc p-values are presented in Tab. III.

E. Cognitive Load (NASA-TLX)

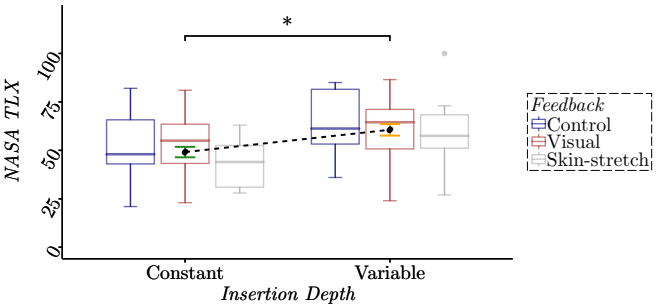

Fig. 9. Experimental results for the NASA TLX. Post-hoc pairwise comparisons of the EMM using Fischer's LSD p-values are indicated as follows: * = $p < 0.05$.

Fig. 9 reports the NASA TLX at constant and varying insertion depth for every feedback modality. The effects of both the feedback modality and the interaction were not significant. However, the effect of the insertion depth was statistically significant ($F(1, 11) = 14.80$, $p = 0.0027$, $\eta^2_{ges} = 0.107$). Specifically, when compared to a fixed insertion depth, participants reported a significantly higher cognitive load score, with a 23.4% (10.50 points) increase (fixed depth: $M = 49.11$, $SD = 16.19$; variable depth: $M = 60.61$, $SD = 17.99$).

F. End-of-experiment Survey

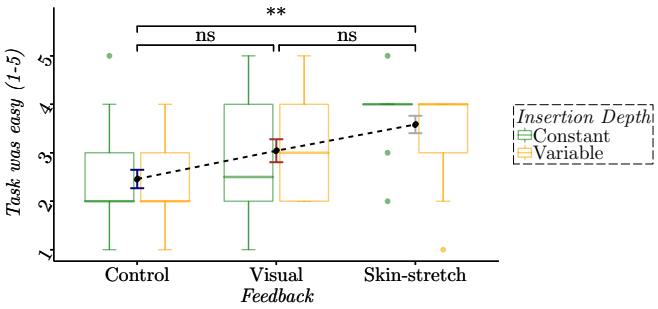

Fig. 10. Experimental results for the Perceived difficulty: "Task was easy" - 5-pt Likert scale (1 - Fully Disagree / 5 - Fully agree). Post-hoc pairwise comparisons of the EMM using Fischer's LSD with ART-C procedure and H-B correction p-values are indicated as follows: ns = $p > 0.05$, ** = $p < 0.01$.

Participants were asked a series of six questions using 5-point bipolar Likert scales (1 meant a strong disagreement while 5 meant a strong agreement).

First, participants were asked if the task was easy to perform for each combination of feedback modality and insertion depth. The results are shown in Fig. 10. Since the data violate the normality assumption, the non-parametric Aligned Rank Transform (ART) [58] procedure was applied, in order to perform a 2RM ANOVA on the aligned and ranked data. The effects of both the insertion depth and the interaction were found to be not significant. However, the test revealed a significant effect of the feedback modality ($F(2, 22) = 5.88$, $p = 0.0089$, $\eta^2_{ges} = 0.189$). The Align Rank Transform for multifactor Contrast (ART-C) [59] procedure was applied prior to performing the post hoc tests. With the visual feedback, participants' ratings were not significantly different than with the skin-stretch feedback or with the control feedback (visual: $M = 3.04$, $SD = 1.16$; skin-stretch: $M = 3.58$, $SD = .88$; control: $M = 2.46$, $SD = .93$). However, participants reported that the task was significantly easier with the skin-stretch feedback compared to the control condition, $p = 0.0065$, with a 45.5% (1.12) increase.

In addition, when asked if the skin-stretch feedback was understandable, participants' ratings were not significantly different between a constant and a varying insertion depth (constant depth: $M = 4.42$, $SD = 0.67$; varying depth: $M = 4.33$, $SD = 0.49$).

Finally, when asked if they experienced any discomfort while wearing the wristband, all 12 of them reported not

feeling any discomfort, and when asked if the device was comfortable, the mean answer was 3.83 ($SD = 1.11$).

V. Discussion

The present study evaluated the suitability of a tactile feedback based on tangential skin-stretch to augment the perception of radial forces applied at the laparoscopic tool-tip and its effectiveness in mitigating the lever effect, which distorts haptic perception in minimally invasive surgery. The proposed feedback was compared against conventional visual feedback and no feedback augmentation in a stiffness discrimination task. Results confirmed the relevance of the experimental protocol and highlighted that the tactile feedback improved performance on both objective and subjective metrics. The results first validate the protocol by showing that augmenting force information—via tactile or visual feedback—significantly increased the success rate compared to the control condition. This finding confirms the relevance of the feedback modalities for this task and the appropriateness of their comparison. More specifically, skin-stretch feedback significantly outperformed the control condition on all metrics except completion time, where no difference was observed. Visual feedback also improved success rate and reduced peak force but showed no effect on confidence or perceived difficulty. In addition, as demonstrated by Nisky *et al.* in [7], the lever effect greatly distorts the haptic perception of forces and leads to a bias in the perceived tissue stiffness, that the present results also highlight. Indeed, under the control condition, varying the insertion depth leads to a significant decrease of the success rate in accurately evaluating samples' stiffness. Moreover, under the control condition as well as with visual or tactile sensory augmentation, all other metrics were significantly negatively impacted. Specifically, with a variable insertion depth, participants applied higher forces, were less confident in their answers, needed more time to complete the task and presented a higher cognitive load. Furthermore, although both feedback modalities increased performance, the tactile feedback outperformed the visual feedback in several occasions. Indeed, in terms of success rate, the performance was significantly better with the tactile feedback at a constant depth. Also, in contrast to the tactile feedback, the visual feedback did not improve confidence, which is a direct indicator of participants' subjective experience. This might explain why the skin-stretch feedback is the only one to reduce the perceived difficulty.

These results are in line with our findings of Saudrais *et al.* [51], which investigated the perception of axial forces. In the present case of radial forces, the results are consistent, i. e. the skin-stretch feedback also significantly outperforms a visual bar-graph feedback. Even though the skin deformation and the applied force are not collinear, the feedback is also highly understandable with no cognitive load increase, regardless of the insertion depth condition. The cognitive cost of the mental rotation required to realign the stimuli is therefore small, which is consistent with the results presented in [60].

The reduction in performance when the insertion depth is variable suggests that the feedback could be improved. In this respect, at varying depth, some participants reported that they were sometimes unsure whether they had indented the samples purely radially. Therefore, an area for improvement would be to enrich the conveyed information, for instance by rendering both normal and tangential tooltip forces using a multi-DoF device, in order to facilitate normal indentation of the samples, albeit at the risk of increasing the cognitive load. Also, considering that skin stiffness can be influenced by various factors including age, temperature, and humidity, it appears pertinent to consider personalizing the feedback to the user.

Interestingly, it can further be noted that under the visual condition, varying the insertion depth had no effect on success rate, as opposed to the control and tactile conditions where a constant insertion depth led to a significant increase in success rate. As several participants reported completely disregarding their haptic perception of forces under the visual condition since it might conflict with the distorted natural haptic feedback, with that feedback modality, the force information might actually be more integrated by sensory substitution rather than augmentation, which would explain the similar success rate regardless the of insertion depth. In other words, with the visual feedback as opposed to the skin-stretch feedback, it appears that the natural haptic feedback is no longer integrated and therefore no longer contributes to the perception of forces. This is in line with the assumption advanced in [49] that using the same sensory channel is more intuitive and that a tactile feedback is therefore better suited to enhancing the force information.

Concerning the participants' performance under the control condition, it may come as a surprise that the success rate was only marginally above the chance level for a few participants, indicating a Weber fraction (WF) slightly below 0.38. Although this value is higher than those reported in the literature, it is not unexpected since this literature primarily focuses on direct palpation performed with the finger. In contrast, in this study, palpation was performed using a tool inserted in a trocar and constrained to radial motion. It introduces significant distortions in stiffness perception, such as the lever effect, the abdominal wall's elasticity, the tool's flexion, and the trocar backlash. Greenwald's *et al.* [61] research on tumor detection in a phantom also revealed similar results, showing that tool-mediated palpation (with or without a trocar) led to significantly lower performance compared to manual palpation, even for tumors of very high relative stiffness, indicating a much higher WF. Future studies will aim to accurately assess this degradation and quantify the improvement provided by the skin stretch feedback, especially in terms of the WF.

In comparison with the literature, Fukuda *et al.* [45] studied the effect on laparoscopic palpation of visual line-graph feedback and a tactile feedback, in the form of a normal force applied to the user's foot. Both yielded a reduction in palpation force, aligning with our study. However, only the visual feedback significantly improved tumor detection in their

research, which diverges from our results that demonstrate an overall superior performance of the tactile feedback over the visual feedback. This disparity might be attributed to the fact that rendering the feedback on the foot instead of in the palpation movement, as done in our study, potentially leads to feedback integration challenges and reduces understandability. The greater sensitivity of the skin to tangential displacement, compared with normal displacement [50] might also explain the improved performance of the skin-stretch feedback.

In addition, the task involved only one comparison set of springs to avoid lengthening the protocol, as laparoscopic surgery is known to lead to fatigue quickly, especially in naive subjects [62], and also to limit the learning effect. The objective was to keep the participants as naïve as possible to assess the intuitive aspect of the device effectively. The investigation of the learning effect will be the subject of future work. In this regard, it is worth noting that contrary to vibrotactile feedback that might eventually lead to desensitization [63], the subjects or the experimenter noted no decrease in sensitivity at the end of the session, although this was not quantified.

Lastly, although the experimental setup is firmly anchored in the medical world, through the use of a realistic tool, a genuine medical trocar, a mock abdominal wall from a professional medical laparoscopy trainer, and a task involving gestures inspired by abdominal wall surgery, it is not a real tissue palpation as the one carried out in [45]. Also, the force sensor used is incompatible with actual laparoscopic surgery, for which a sensor meeting, among others, the size and sterilization requirements, such as those proposed in [31], [64], [65], would be necessary. The present study involved a guided task and was conducted under simplified conditions, due to the need to create a controlled environment. Future work will focus on extending this work to a more realistic scenario, incorporating a greater range of stiffness comparisons, possibly using silicone phantoms or animal tissue. In addition, the current setup assumes a fixed camera viewpoint, whereas in actual laparoscopic procedures, camera motion can alter visual feedback and affect task performance, a factor that will also need to be considered in future investigations.

Additionally, the study deliberately involved inexperienced participants to avoid experience bias as it correlates to better stiffness discrimination [66]. Nevertheless, it would be necessary to validate these findings with experienced participants, given that they represent the ultimate end-users.

REFERENCES

[1] V. Velanovich, "Laparoscopic vs open surgery: A preliminary comparison of quality-of-life outcomes," *Surgical Endoscopy*, vol. 14, no. 1, pp. 16–21, 2000.

[2] S. Schostek, M. O. Schurr, and G. F. Buess, "Review on aspects of artificial tactile feedback in laparoscopic surgery," *Medical Engineering and Physics*, vol. 31, no. 8, pp. 887–898, 2009.

[3] E. P. Westebring – van der Putten, R. H. M. Goossens, *et al.*, "Haptics in minimally invasive surgery – a review," *Minimally Invasive Therapy and Allied Technologies*, vol. 17, no. 1, pp. 3–16, 2008.

[4] P. Dubois, Q. Thommen, and A. Jambon, "In vivo measurement of surgical gestures," *IEEE Transactions on Biomedical Engineering*, vol. 49, no. 1, pp. 49–54, 2002.

[5] P. Lamata, E. Gomez, *et al.*, "Understanding Perceptual Boundaries in Laparoscopic Surgery," *IEEE Transactions on Biomedical Engineering*, vol. 55, no. 3, pp. 866–873, 2008.

[6] G. Picod, A. C. Jambon, *et al.*, "What can the operator actually feel when performing a laparoscopy?" *Surgical Endoscopy*, vol. 19, no. 1, pp. 95–100, 2005.

[7] I. Nisky, F. Huang, *et al.*, "Perception of Stiffness in Laparoscopy – the Fulcrum Effect," *Studies in health technology and informatics*, vol. 173, p. 313, 2012.

[8] P. Joice, G. B. Hanna, and A. Cuschieri, "Errors enacted during endoscopic surgery - A human reliability analysis," *Applied Ergonomics*, vol. 29, no. 6, pp. 409–414, 1998.

[9] J. Rosen, B. Hannaford, *et al.*, "Force controlled and teleoperated endoscopie grasper for minimally invasive surgery-experimental performance evaluation," *IEEE Transactions on Biomedical Engineering*, vol. 46, no. 10, pp. 1212–1221, 1999.

[10] M. V. Ottermo, M. Vstedal, *et al.*, "The role of tactile feedback in laparoscopic surgery," *Surgical Laparoscopy Endoscopy and Percutaneous Techniques*, vol. 16, no. 6, pp. 390–400, 2006.

[11] J. O. Perreault and C. G. Cao, "Effects of vision and friction on haptic perception," *Human Factors*, vol. 48, no. 3, pp. 574–586, 2006.

[12] W. Bergmann Tiest and A. Kappers, "Cues for Haptic Perception of Compliance," *IEEE Transactions on Haptics*, vol. 2, no. 4, pp. 189–199, 2009.

[13] E. Fakhoury, P. R. Culmer, and B. Henson, "The effect of indentation force and displacement on visual perception of compliance," *IEEE World Haptics Conference*, pp. 88–93, 2015.

[14] S. B. Archer, D. W. Brown, *et al.*, "Bile duct injury during laparoscopic cholecystectomy: Results of a national survey," *Annals of Surgery*, vol. 234, no. 4, pp. 549–559, 2001.

[15] S. Adamsen, O. Hansen, *et al.*, "Bile duct injury during laparoscopic cholecystectomy: a prospective nationwide series," *Journal of the American College of Surgeons*, vol. 184, no. 6, p. 571—578, 1997.

[16] L. W. Way, L. Stewart, *et al.*, "Causes and Prevention of Laparoscopic Bile Duct Injuries: Analysis of 252 Cases from a Human Factors and Cognitive Psychology Perspective," *Annals of Surgery*, vol. 237, no. 4, pp. 460–469, 2003.

[17] A. R. Lanfranco, A. E. Castellanos, *et al.*, "Robotic Surgery: A Current Perspective," *Annals of Surgery*, vol. 239, no. 1, pp. 14–21, 2004.

[18] F. M. Melfi and A. Mussi, "Robotically Assisted Lobectomy: Learning Curve and Complications," *Thoracic Surgery Clinics*, vol. 18, no. 3, pp. 289–295, 2008.

[19] S. W. Wong, Z. H. Ang, *et al.*, "Robotic colorectal surgery and ergonomics," *Journal of Robotic Surgery*, vol. 16, no. 2, pp. 241–246, 2022.

[20] F. Schmitt, J. Sulub, *et al.*, "Using comanipulation with active force feedback to undistort stiffness perception in laparoscopy," in *2019 IEEE International Conference on Robotics and Automation*, 2019, pp. 3902–3908.

[21] A. J. Spiers, S. Baillie, *et al.*, "Negating the fulcrum effect in manual laparoscopic surgery: Investigating skill acquisition with a haptic simulator," *International Journal of Medical Robotics and Computer Assisted Surgery*, vol. 13, no. 4, pp. 13–15, 2017.

[22] C. C. Alleblas, M. P. Vleugels, and T. E. Nieboer, "Ergonomics of laparoscopic graspers and the importance of haptic feedback: the surgeons' perspective," *Gynecological Surgery*, vol. 13, no. 4, pp. 379–384, 2016.

[23] C. C. Alleblas, M. P. Vleugels, *et al.*, "Performance of a Haptic Feedback Grasper in Laparoscopic Surgery: A Randomized Pilot Comparison With Conventional Graspers in a Porcine Model," *Surgical Innovation*, vol. 26, no. 5, pp. 573–580, 2019.

[24] M. E. Aguirre, K. D. Kommuri, *et al.*, "Multi-Modal Mechanism for Enhancing Haptics and Safety in Handheld Surgical Grasping," in *2022 IEEE Haptics Symposium (HAPTICS)*. IEEE, mar 2022, pp. 1–6.

[25] W. Othman, K. E. Vandyck, *et al.*, "Stiffness Assessment and Lump Detection in Minimally Invasive Surgery Using In-House Developed Smart Laparoscopic Forceps," *IEEE Journal of Translational Engineering in Health and Medicine*, vol. 10, no. June, pp. 1–10, 2022.

[26] K. A. Kaczmarek, "Sensory Augmentation and Substitution," in *Biomedical Engineering Fundamentals*, J. D. Bronzino, Ed. CRC Press, 2006, vol. 5, no. 1, pp. 1263–1272.

[27] K. H. Sienko, R. D. Seidler, *et al.*, "Potential mechanisms of sensory augmentation systems on human balance control," *Frontiers in Neurology*, vol. 9, 2018.

[28] M. O. Ernst and M. S. Banks, "Humans integrate visual and haptic information in a statistically optimal fashion," *Nature*, vol. 415, no. 6870, pp. 429–433, jan 2002.

[29] T. Howard and J. Szewczyk, "Visuo-haptic feedback for 1-D Guidance in laparoscopic surgery," in *Proceedings of the IEEE RAS and EMBS International Conference on Biomedical Robotics and Biomechatronics*, 2014, pp. 58–65.

[30] E. Afshari, H. Sarkhosh, and S. Najarian, "A novel tactile probe with medical and surgical applications," *Sensor Review*, vol. 37, no. 4, pp. 404–409, 2017.

[31] A. S. Naidu, R. V. Patel, and M. D. Naish, "Low-Cost Disposable Tactile Sensors for Palpation in Minimally Invasive Surgery," *IEEE/ASME Transactions on Mechatronics*, vol. 22, no. 1, pp. 127–137, 2017.

[32] C. Wiederer, M. Fröhlich, and M. W. Strohmayr, "Improving tactile sensation in laparoscopic surgery by overcoming size restrictions," *Current Directions in Biomedical Engineering*, vol. 1, no. 1, pp. 135–139, 2015.

[33] T. Howard and J. Szewczyk, "Assisting control of forces in laparoscopy using tactile and visual sensory substitution," *Mechanisms and Machine Science*, vol. 39, pp. 151–164, 2016.

[34] R. Hoskins, J. Wang, and C. G. Cao, "Use of stochastic resonance methods for improving laparoscopic surgery performance," *Surgical Endoscopy*, vol. 30, no. 10, pp. 4214–4219, 2016.

[35] R. E. Schoonmaker and C. G. Cao, "Vibrotactile Feedback Enhances Force Perception in Minimally Invasive Surgery," in *Proceedings of the Human Factors and Ergonomics Society Annual Meeting*, vol. 50, no. 10, 2006, pp. 1029–1033.

[36] Y. Tanaka, T. Nagai, *et al.*, "Tactile sensing system including bidirectionality and enhancement of haptic perception by tactile feedback to distant part," *2013 World Haptics Conference, WHC 2013*, pp. 145–150, 2013.

[37] B. Weber, M. Sagardia, *et al.*, "Visual, vibrotactile, and force feedback of collisions in virtual environments: Effects on performance, mental workload and spatial orientation," in *Virtual Augmented and Mixed Reality. Designing and Developing Augmented and Virtual Environments*, 2013, pp. 241–250.

[38] T. Fukuda, Y. Tanaka, *et al.*, "A pneumatic tactile ring for instantaneous sensory feedback in laparoscopic tumor localization," *IEEE Transactions on Haptics*, vol. 11, no. 4, pp. 485–497, 2018.

[39] H. H. Ly, Y. Tanaka, and M. Fujiwara, "SuP-Ring: A pneumatic tactile display with substitutional representation of contact force components using normal indentation," *International Journal of Medical Robotics and Computer Assisted Surgery*, vol. 17, no. 6, pp. 0–2, 2021.

[40] S. B. Schorr, Z. F. Quek, *et al.*, "Tactor-Induced Skin Stretch as a Sensory Substitution Method in Teleoperated Palpation," *IEEE Transactions on Human-Machine Systems*, vol. 45, no. 6, pp. 714–726, 2015.

[41] Y. Mo, A. Song, and H. Qin, "Analysis and Performance Evaluation of a 3-DOF Wearable Fingertip Device for Haptic Applications," *IEEE Access*, vol. 7, pp. 170 430–170 441, 2019.

[42] Z. F. Quek, W. R. Provancher, and A. M. Okamura, "Evaluation of Skin Deformation Tactile Feedback for Teleoperated Surgical Tasks," *IEEE Transactions on Haptics*, vol. 12, no. 2, pp. 102–113, 2019.

[43] F. Chinello, M. Malvezzi, *et al.*, "A modular wearable finger interface for cutaneous and kinesthetic interaction: Control and evaluation," *IEEE Transactions on Industrial Electronics*, vol. 67, no. 1, pp. 706–716, 2020.

[44] Z. F. Quek, S. B. Schorr, *et al.*, "Augmentation Of Stiffness Perception With a 1-Degree-of-Freedom Skin Stretch Device," *IEEE Transactions on Human-Machine Systems*, vol. 44, no. 6, pp. 731–742, 2014.

[45] T. Fukuda, Y. Tanaka, *et al.*, "Visual and tactile feedback for a direct-manipulating tactile sensor in laparoscopic palpation," *International Journal of Medical Robotics and Computer Assisted Surgery*, vol. 14, no. 2, pp. 1–13, 2018.

[46] Y. Tanaka, T. Nagai, *et al.*, "Lump detection with tactile sensing system including haptic bidirectionality," *World Automation Congress Proceedings*, pp. 77–82, 2014.

[47] F. Chinello, C. Pacchierotti, *et al.*, "Design of a wearable skin stretch cutaneous device for the upper limb," in *2016 IEEE Haptics Symposium*, 2016, pp. 14–20.

[48] A. Campanelli, M. Tiboni, *et al.*, "Innovative Multi Vibrotactile-Skin Stretch (MuViSS) haptic device for sensory motor feedback from a robotic prosthetic hand," *Mechatronics*, vol. 99, p. 103161, may 2024.

[49] S. B. Schorr, Z. F. Quek, *et al.*, "Sensory substitution via cutaneous skin stretch feedback," in *2013 IEEE International Conference on Robotics and Automation*, 2013, pp. 2341–2346.

[50] J. Biggs and M. A. Srinivasan, "Tangential versus normal displacements of skin: Relative effectiveness for producing tactile sensations," in *10th Symposium on Haptic Interfaces for Virtual Environment and Teleoperator Systems*, 2002, pp. 121–128.

[51] C. Saudrais, B. Bayle, *et al.*, "Skin-stretch haptic feedback augmentation improves performance in a simulated laparoscopic palpation task," *IEEE Trans. Haptics*, vol. 17, no. 4, p. 578–590, Oct. 2024.

[52] B. T. Gleeson, C. A. Stewart, and W. R. Provancher, "Improved tactile shear feedback: Tactor design and an aperture-based restraint," *IEEE Transactions on Haptics*, vol. 4, no. 4, pp. 253–262, 2011.

[53] A. K. Golahmadi, D. Z. Khan, *et al.*, "Tool-tissue forces in surgery: A systematic review," *Annals of Medicine and Surgery*, vol. 65, no. March, p. 102268, 2021.

[54] S. G. Hart and L. E. Staveland, *Development of NASA-TLX (Task Load Index): Results of Empirical and Theoretical Research*, ser. Human Mental Workload. Elsevier, 1988, vol. 52.

[55] B. G. Tabachnick and L. S. Fidell, "Using multivariate statistics (5th ed.)," Boston, MA, 2007.

[56] R Core Team, *R: A Language and Environment for Statistical Computing*, R Foundation for Statistical Computing, Vienna, Austria, 2022.

[57] J. Hsu, *Multiple Comparisons*. Chapman and Hall/CRC, 1996.

[58] J. O. Wobbrock, L. Findlater, *et al.*, "The Aligned Rank Transform for nonparametric factorial analyses using only ANOVA procedures," in *Conference on Human Factors in Computing Systems*, 2011, pp. 143–146.

[59] L. A. Elkin, M. Kay, *et al.*, "An aligned rank transform procedure for multifactor contrast tests," in *The 34th Annual ACM Symposium on User Interface Software and Technology*, 2021, p. 754–768.

[60] B. T. Gleeson and W. R. Provancher, "Mental rotation of tactile stimuli: Using directional haptic cues in mobile devices," *IEEE Transactions on Haptics*, vol. 6, no. 3, pp. 330–339, 2013.

[61] D. Greenwald, C. G. Cao, and E. W. Bushnell, "Haptic detection of artificial tumors by hand and with a tool in a mis environment," *IEEE Transactions on Haptics*, vol. 5, no. 2, pp. 131–138, 2012.

[62] R. Berguer, D. L. Forkey, and W. D. Smith, "Ergonomic problems associated with laparoscopic surgery," *Surgical Endoscopy*, vol. 13, no. 5, pp. 466–468, may 1999.

[63] P. Chaubey, T. Rosenbaum-Chou, *et al.*, "Closed-Loop Vibratory Haptic Feedback in Upper-Limb Prosthetic Users," *JPO Journal of Prosthetics and Orthotics*, vol. 26, no. 3, pp. 120–127, jul 2014.

[64] P. Wang, S. Zhang, *et al.*, "Smart laparoscopic grasper integrated with fiber Bragg grating based tactile sensor for real-time force feedback," *Journal of Biophotonics*, vol. 15, no. 5, may 2022.

[65] Y. Tanaka, T. Fukuda, *et al.*, "Tactile sensor using acoustic reflection for lump detection in laparoscopic surgery," *International Journal of Computer Assisted Radiology and Surgery*, vol. 10, no. 2, pp. 183–193, 2015.

[66] N. Forrest, S. Baillie, *et al.*, "A comparative study of haptic stiffness identification by veterinarians and students," *IEEE Transactions on Haptics*, vol. 4, no. 2, pp. 78–87, 2011.